AN IMPROVED VARIABLE SAMPLE SIZE AND SAMPLING INTERVAL *S* CONTROL CHART

SEE MAY YEN

UNIVERSITI SAINS MALAYSIA

2018

AN IMPROVED VARIABLE SAMPLE SIZE AND SAMPLING INTERVAL *S* CONTROL CHART

by

SEE MAY YEN

Thesis submitted in fulfillment of the requirements for the degree of Master of Science

May 2018

ACKNOWLEDGEMENT

First and foremost, I wish to express my sincere appreciation to my supervisor, Professor Michael Khoo Boon Chong for his enthusiasm, patience and inspiration in guiding me until the completion of this thesis. He is willing to share his insight and knowledge with me. Besides that, he has also recruited me as a research assistant for 11 months using his research grant, which has provided me with some financial support.

I would like to acknowledge the Dean of the School of Mathematical Sciences, USM, Professor Hailiza Kamarulhaili, and her deputies Associate Professor Mohd. Tahir Ismail and Associate Professor Ong Hong Choon. Besides that, I would also like to express my gratitude to the lecturers and staff of the faculty, for their constant assistance and guidance. They have assisted me in one way or another to complete this research.

I am thankful to the USM librarians for their assistance. They have helped me to source for research materials from journals and reference books. With their help, I am able to access the library's resources easily and effectively, where the information related to this study is searched electronically via the online databases.

I am thankful to be a recipient of the MyMaster scholarship under the MyBrain15 program of the Ministry of Higher Education (MOHE). This scholarship covers my tuition fees.

I am indebted to my family members, especially my father, for providing me with the opportunity to further my study. They have always supported me in whatever decisions that I made.

Last but not least, I also wish to express my appreciation to my friends, especially Ms. Teh Jiun Ling, Ms. Ng Ying Yiing, Ms. Chua Jit-Ni Ginny, Ms. Lim Yong Hui and Ms. Kh’ng Xin Yi for their useful suggestions and support.

TABLE OF CONTENTS

LIST OF TABLES

LIST OF FIGURES

LIST OF ABBREVIATIONS

ARL	Average run length
ATS	Average time to signal
CL	Center line
cdf	Cumulative distribution function
EARL	Expected average run length
EATS	Expected average time to signal
EWMA	Exponentially weighted moving average
pdf	Probability density function
SPC	Statistical Process Control
SQC	Statistical Quality Control
tpm	Transition probability matrix
UCL	Upper control limit
VSI	Variable sampling interval
VSS	Variable sample size
VSSI	Variable sample size and sampling interval
$VSSI_t$	Improved variable sample size and sampling interval

LIST OF NOTATIONS

K	Control limit constant of the EWMA *S* chart
Ω	Finite state space
$\mathbf{I}$	Identity matrix
μ_0	In-control population mean
$\boldsymbol{\pi}$	Initial probability vector
$\boldsymbol{\alpha}$	Initial probability vector for the transient states of the VSSI *S* chart
X_{ij}	jth observation in the ith sample
$f(\lambda)$	pdf of the shift size, λ
σ_0	In-control population standard deviation
σ_1	Out-of-control population standard deviation
σ_S	Population standard deviation of the sample standard deviation
n_0	Specified desired average sample size when the process is in-control
n_1	Small sample size
n_2	Large sample size
$n(i)$	Sample size for the ith sample
t_0	Specified desired average sampling interval when the process is in-control
t_1	Long sampling interval for the VSSI *S*, modified VSSI *S* and VSSI_t S charts
t_2	Short sampling interval for the VSSI *S* and modified VSSI *S* charts or moderate sampling interval for the VSSI_t S chart
t_3	Short sampling interval for the VSSI_t S chart

$t(i)$	Sampling interval between the ith and $(i+1)$th samples
p	Probability in which a single point falls above the UCL
b_1	Proportion of time spent using (t_1, n_1)
b_2	Proportion of time spent using (t_2, n_2)
$\bar{X}$	Sample mean
R	Sample range
S	Sample standard deviation
S^2	Sample variance
λ	Shift size in the process standard deviation
$\lambda_{\min}$	Minimum shift size in the process standard deviation
$\lambda_{\max}$	Maximum shift size in the process standard deviation
λ^*	Smoothing constant of the EWMA *S* chart
α	Size of Type-I error
β	Size of Type-II error
$\mathbf{P}$	Transition probability matrix of the $\mathrm{VSSI_t}$ S chart with the absorbing state
$\mathbf{Q}$	Transition probability matrix for the transient states of the VSSI *S*, EWMA *S* and $\mathrm{VSSI_t}$ S charts
$\mathbf{Q}_*$	Transition probability matrix for the transient states of the modified VSSI *S* chart
k_0	UCL of the $\mathrm{VSSI_t}$ S chart
L	UCL of the modified VSSI *S* chart
L_1	UCL of the VSSI *S* chart when the sample size is n_1
L_2	UCL of the VSSI *S* chart when the sample size is n_2

w	Upper warning limit of the modified VSSI S chart
w_1	Upper warning limit of the VSSI S chart when the sample size is n_1
w_2	Upper waning limit of the VSSI S chart when the sample size is n_2
w_1 / w_2	Upper warning limits of the VSSI_t S chart, where $w_1 < w_2$
$\mathbf{t}$	Vector of sampling intervals for the VSSI S chart
$\mathbf{t}_*$	Vector of sampling intervals for the modified VSSI S chart
$\mathbf{b}$	Vector of starting probabilities

CARTA KAWALAN *S* DENGAN SAIZ SAMPEL DAN SELANG PENSAMPELAN BOLEH UBAH YANG DITAMBAHBAIK

ABSTRAK

Carta sisihan piawai atau carta *S* digunakan untuk memantau sisihan piawai proses. Dalam tesis ini, beberapa ciri carta *S* telah diubahsuai untuk meningkatkan kepekaan carta tersebut terhadap anjakan kecil dan sederhana dalam sisihan piawai proses. Carta baru ini dikenali sebagai carta *S* dengan saiz sampel dan selang pensampelan boleh ubah yang ditambahbaik ($\mathrm{VSSI_t}$). Reka bentuk dan pembinaan carta $\mathrm{VSSI_t}$ S adalah berdasarkan idea carta $\bar{X}$ dengan saiz sampel dan selang pensampelan boleh ubah yang ditambahbaik ($\mathrm{VSSI_t}$) yang dicadangkan oleh Noorossana et al. pada tahun 2016. Carta $\mathrm{VSSI_t}$ $\bar{X}$ menambahbaik kecekapan carta-carta jenis $\bar{X}$ dalam pengesanan anjakan kecil dan sederhana dalam min proses. Carta $\mathrm{VSSI_t}$ S menggunakan dua saiz sampel and tiga selang persampelan. Pendekatan rantai Markov digunakan dalam reka bentuk carta $\mathrm{VSSI_t}$ S untuk penilaian prestasi masa purata untuk berisyarat (ATS) dan jangkaan masa purata untuk berisyarat (EATS) carta tersebut. Prestasi ATS dan EATS carta $\mathrm{VSSI_t}$ S optimum dibandingkan dengan prestasi sepadan carta *S* purata bergerak berpemberat eksponen (EWMA) optimum, carta *S* dengan saiz sampel dan selang pensampelan boleh ubah (VSSI) yang diubahsuai optimum dan carta *S* piawai. Nilai ATS dan EATS bagi semua carta dikira dengan menggunakan program MATLAB. Program-program simulasi dalam perisian Sistem Analisis Berstatistik (SAS) juga digunakan untuk mengesahkan kejituan nilai-nilai ATS dan EATS yang dikira melalui MATLAB. Didapati bahawa carta $\mathrm{VSSI_t}$ S adalah lebih baik daripada carta-carta *S*

piawai, VSSI *S* yang diubahsuai dan EWMA *S* dalam pengesanan anjakan sederhana dan besar dalam sisihan piawai proses, daripada segi kriteria ATS dan EATS. Suatu contoh ilustrasi diberikan untuk menunjukkan pembinaan carta $\text{VSSI}_t\ S$.

AN IMPROVED VARIABLE SAMPLE SIZE AND SAMPLING INTERVAL *S* CONTROL CHART

ABSTRACT

The standard deviation chart or *S* chart is used to monitor the process standard deviation. In this thesis, some of the features of the *S* chart are altered to increase the chart's sensitivity towards small and moderate shifts in the process standard deviation. This new chart for monitoring the process standard deviation is known as the improved variable sample size and sampling interval (VSSI_t) *S* chart. The design and construction of the VSSI_t *S* chart is based on the idea of the improved variable sample size and sampling interval (VSSI_t) $\bar{X}$ chart proposed by Noorossana et al. in 2016. The VSSI_t $\bar{X}$ chart improves the efficiency of the $\bar{X}$-type charts in detecting small and moderate shifts in the process mean. The VSSI_t *S* chart uses two sample sizes and three sampling intervals. The Markov chain approach is employed in the design of the VSSI_t *S* chart for evaluating the chart's average time to signal (ATS) and expected average time to signal (EATS) performances. The ATS and EATS performances of the optimal VSSI_t *S* chart are compared with that of the optimal exponentially weighted moving average (EWMA) *S*, optimal modified variable sample size and sampling interval (VSSI) *S* and standard *S* charts. The ATS and EATS values of all the charts are computed using the MATLAB programs. The simulation programs in the Statistical Analysis System (SAS) software are also used to verify the accuracy of the ATS and EATS values computed via MATLAB. It is found that the VSSI_t *S* chart is superior to the

standard *S*, modified VSSI *S* and EWMA *S* charts, in detecting moderate and large shifts in the process standard deviation, in terms of the ATS and EATS criteria. An illustrative example is given to show the construction of the $\mathrm{VSSI}_t\ S$ chart.

CHAPTER 1

INTRODUCTION

1.1 Statistical Quality Control (SQC)

Nowadays, the quality of a product produced by a manufacturer or service provided by a service provider is being given more emphasis by consumers. Quality is defined as fitness for use that fulfils customers' expectations and requirements. In the modern definition, "quality" is inversely proportional to variability (Montgomery, 2013). There are several ways to describe and evaluate the quality of a product or service.

Quality control is a regulatory process to measure the performance of a product by comparing it with established standards so that corrective actions are taken if required (Besterfield, 1979). There are four essential techniques used in a quality control program (Western Electric Company, 1958):

1) Process Capability Study.
2) Process Control Chart.
3) Statistical Sampling Inspection.
4) Statistical Design of Experiment.

Process capability study is a basic technique used for analysing data to acquire information about the behaviour of a process. A process control chart is used to improve the process quality of a manufacturing process. Statistical sampling inspection is used as a scientific basis to inspect the product while statistical design of experiment uses statistical tests for analysing whether a significant effect exists in a process.

Statistical techniques are employed in quality control to identify the trouble spots and their causes. Statistical Quality Control (SQC) is a collection of tools for analysing and interpreting data to solve a particular quality problem (Besterfield, 1979). SQC is used with the aim of making the quality characteristics of a process falling within the specified boundaries in a manufacturing operation (Western Electric Company, 1958).

Before the late 1920s, quality control deals with the inspection of mainly 100% of all the products produced. Walter A. Shewhart of the Bell Telephone Laboratories developed the SQC concept in 1924. This concept is usually considered as the formal beginning of Statistical Quality Control (SQC) (Montgomery, 2013). Harold F. Dodge and Harry G. Romig, both from the Bell Telephone Laboratories proposed the concept of acceptance sampling plans in the later part of the 1920s. These plans are considered as alternatives to 100% inspection. After World War II, the SQC concepts have been used extensively due to the higher demand of products with higher quality (Shirland, 1993).

Improvements and extensions of the SQC techniques have been extensively carried out during the years after World War II. Several consultants from the United States were hired by Japanese companies to guide them to recover from the destruction due to the war by using SQC techniques. W. Edwards Deming and Joseph Juran emphasized that SQC comprises a set of tools used in the implementation of management principles (Shirland, 1993). SQC concepts have also led to the development of several international standards, such as sampling procedures and tables for inspection by attributes (ANSI/ASQCZ1.4), ISO 9000 and ISO 9001 (Crossley, 2000; Hoyle, 2001 and Montgomery, 2013).

1.2 Control Charting Techniques

Control chart is one of the seven tools (also known as the magnificent seven) in Statistical Process Control (SPC). SPC is a collection of problem solving tools to achieve process stability and improve process capability by reducing variability (Montgomery, 2013). Burr (1976) pointed out that the purpose of using control charts is to analyse past data for controlling and comparing the observed results against a population whose parameter or parameters are known.

Besterfield (1979) presented a procedure to establish a pair of control charts for the mean, $\bar{X}$ and range, R as follows:

Step 1. Select the quality characteristic.

Step 2. Choose the rational subgroup.

Step 3. Collect the data.

Step 4. Compute the trial control limits.

Step 5. Establish the revised control limits.

A quality characteristic that can be measured in numbers or on a continuous scale consists of variables data. Examples of such quality characteristics are length, mass, time, electrical current, temperature and luminous intensity. Rational subgrouping is a collection of sample data that are plotted on a control chart. Some guidelines for deciding on the sample size to be used are as follows (Besterfield, 1979):

1) The control limits are closer to the center line when the sample size increases. This makes the control chart to be more sensitive to small variation in the process average.
2) The inspection cost per sample increases as the sample size increases.
3) A small sample is used to minimize the destruction of expensive products.

4) The ease of computation based on a sample size of five is no longer valid as computers are being used widely.

5) According to statistical basis, the distribution of the sample average when samples are taken from non-normal populations is nearly normal for samples of size four or more each, and there are at least 20 – 25 samples altogether used in estimating the grand sample average.

6) The *S* chart is used instead of *R* chart when the sample size exceeds ten for the control of the dispersion.

A collection of the Phase-I data with a minimum of 25 samples is used for an accurate computation of the trial limits of control charts. Usually the limits are set as ±3 standard deviations from the center line. The Phase-I samples are plotted on the chart along with the trial limits and center line computed. The trial limits are revised if necessary, when a sample point plots beyond the limits.

1.3 Objectives of the Thesis

The objectives are as follow:

(i) To propose the VSSI_t S control chart, where the Markov chain approach is used to optimally design the chart.

(ii) To compare the average time to signal (ATS) and expected average time to signal (EATS) performances of the optimal VSSI_t S chart with that of other existing *S*-type charts.

1.4 Organization of the Thesis

This thesis is organized as follows: Explanations on Statistical Quality Control (SQC), control charting techniques and objectives of the thesis are given in

Chapter 1. A review on existing upper-sided *S*-type charts is given in Chapter 2. In Chapter 3, the $\mathrm{VSSI_t}\ S$ chart is presented, together with discussions on the Markov chain model and an optimal design of the chart. The computation of the optimal parameters of the $\mathrm{VSSI_t}\ S$ chart is described in Chapter 4 together with comparisons of ATS and EATS results of the $\mathrm{VSSI_t}\ S$ and existing *S*-type charts. In addition, this chapter also gives an illustrative example to show the implementation of the $\mathrm{VSSI_t}\ S$ chart in a real situation. Lastly, conclusions and suggestions for future research are presented in Chapter 5.

CHAPTER 2

LITERATURE REVIEW

2.1 Introduction

In this chapter, a review on several *S*-type charts is presented. As the proposed VSSI_t *S* chart deals only with an increasing shift in the process standard deviation, only the upper-sided *S*-type charts are reviewed. Note that the detection of an increasing shift in the process standard deviation (by using an upper-sided *S*-type chart) is more important than that of a decreasing shift in the process standard deviation (by using a lower-sided *S*-type chart) as the former indicates a process deterioration while the latter indicates a process improvement. As this thesis deals only with the upper-sided *S*-type chart, for brevity, the phrase "upper-sided" will be omitted in the names of all *S*-type charts discussed in this thesis from now on. Sections 2.2, 2.3 and 2.4 provide discussions on the existing standard *S*, VSSI *S* and EWMA *S* charts, respectively.

2.2 Standard *S* Chart

The standard *S* chart is one of the Shewhart-type control charts. It is used for detecting shifts in the process standard deviation, where it is able to detect large shifts quickly. However, like the Shewhart $\bar{X}$ chart, the standard *S* chart is insensitive in detecting small and moderate shifts in the process standard deviation (Kuo and Lee, 2013).

Let X_{ij} be the *j*th observation in the *i*th random sample (for $i = 1, 2, \ldots$) of size n_0 (i.e. $j = 1, 2, \ldots, n_0$), for quality characteristic *X*. The sample mean $\bar{X}_i$ and the sample standard deviation S_i of the ith sample are computed as (Rakitzis and Antzoulakos, 2011)

$$\bar{X}_i = \frac{1}{n_0}\sum_{j=1}^{n_0} X_{ij} \tag{2.1}$$

and

$$S_i = \sqrt{\frac{1}{n_0 - 1}\sum_{j=1}^{n_0}\left(X_{ij} - \bar{X}_i\right)^2}, \tag{2.2}$$

respectively (Montgomery, 2013).

Assume that X_{ij} follows a normal distribution with mean μ_0 and standard deviation σ, i.e. $X_{ij} \sim N\left(\mu_0, \sigma^2\right)$. Note that $\sigma = \sigma_0$ when the process standard deviation is in-control while $\sigma = \sigma_1$ when the process standard deviation is out of-control, where $\sigma_1 = \lambda\sigma_0$. When $0 < \lambda < 1$, a decreasing shift in the process standard deviation occurs, while an increasing shift in the process standard deviation occurs when $\lambda > 1$. The process standard deviation is in-control when $\lambda = 1$. It is also assumed that the sample standard deviations, S_i, for $i = 1, 2, \ldots$, are independent of one another.

In the construction of the standard S chart, Montgomery (2013) used the traditional $\pm 3\sigma_S$ limits, where σ_S is the standard deviation of S_i. However, Grant and Leavenworth (1980) and Ryan (2011) suggested the use of probability limits due to the skewness of the distribution of the sample standard deviation statistic, S_i. This is coupled by the fact that S_i is not an unbiased estimator of the process standard deviation, σ (Zhang et al., 2005). The upper-sided S chart is used to detect increasing shifts in the process standard deviation. The upper probability limit of the S chart is (Rakitzis and Antzoulakos, 2016)

$$\text{UCL} = \sigma_0 \sqrt{\frac{\chi^2_{n_0-1;\alpha}}{n_0 - 1}}\,, \tag{2.3}$$

where α is the size of the Type-I error while $\chi^2_{n_0-1,\alpha}$ is the $100(1-\alpha)$th percentile of the chi-square distribution with $n_0 - 1$ degrees of freedom.

The average run length (ARL) is the average number of sample points plotted on a control chart until an out-of-control signal is issued by the chart. The ARL is commonly used as a performance measure of a chart. When the process is in-control, the ARL values will be large. Otherwise, the ARL values will be small (Zimmer et al., 2000). For a Shewhart-type chart, such as the standard *S* chart, the ARL is given by (Montgomery, 2013)

$$\text{ARL} = \frac{1}{p}, \tag{2.4}$$

where p is the probability that a single point, S_i, falls above the UCL. The value of p for the *S* chart is obtained as (Rakitzis and Antzoulakos, 2016)

$$p = 1 - F_{\chi^2_{n_0-1}}\left(\frac{(n_0-1)UCL^2}{(\lambda\sigma_0)^2}\right), \tag{2.5}$$

where $F_{\chi^2_{n_0-1}}(\cdot)$ is the cumulative distribution function (cdf) of the chi-square distribution with $n_0 - 1$ degrees of freedom. Note that when $\lambda = 1$, the in-control ARL (ARL_0) is obtained while the out-of-control ARL (ARL_1) is computed when $\lambda > 1$.

The expected average run length (EARL) of the *S* chart is obtained as (Huh, 2014)

$$\text{EARL} = E\left[\text{ARL}(\lambda)\right] = \int_{\lambda_{\min}}^{\lambda_{\max}} \text{ARL}(\lambda)\, f(\lambda)\, d\lambda\,, \tag{2.6}$$

where $f(\lambda)$ denotes the probability density function (pdf) of the shift size, λ, while $\text{ARL}(\lambda)$ is obtained from Equation (2.4). In Equation (2.4), p is a function of λ, as shown in Equation (2.5). It is assumed that the shift size, λ follows a uniform distribution on the interval $(\lambda_{\min}, \lambda_{\max})$, i.e. $\lambda \sim U(\lambda_{\min}, \lambda_{\max})$, where $\lambda_{\min}$ and $\lambda_{\max}$ are the minimum and maximum shift sizes, respectively, in the interval $(\lambda_{\min}, \lambda_{\max})$. Consequently,

$$f(\lambda) = \frac{1}{\lambda_{\max} - \lambda_{\min}}. \tag{2.7}$$

2.3 Variable Sample Size and Sampling Interval (VSSI) *S* Chart

Rakitzis and Antzoulakos (2011) presented a VSSI *S* chart. They used the large sample size (n_2) and short sampling interval (t_2) for taking the first sample $(i = 1)$ when no information about the process is available so that initial problems in the process can be detected quickly. Rakitzis and Antzoulakos (2011) defined the adaptive function as follows:

$$\left(t(i+1), n(i+1)\right) = \begin{cases} (t_1, n_1) \text{ if the threshold limit } w_j \text{ is used for sample } i \text{ and } S_i < w_j \\ (t_2, n_2) \text{ if the limits } w_j \text{ and } L_j \text{ are used for sample } i \text{ and } w_j < S_i < L_j \end{cases},$$

for $i = 1, 2, \ldots$ and $j = 1$ if $\left(t(i), n(i)\right) = (t_1, n_1)$, while $j = 2$ if $\left(t(i), n(i)\right) = (t_2, n_2)$. Here t_1 and t_2 represent the long and short sampling intervals, respectively, while n_1 and n_2 denote the small and large sample sizes, respectively. Note that $t(i+1)$ specifies the sampling interval between the ith and $(i+1)$th samples, while $n(i+1)$ denotes the sample size for the $(i+1)$th sample. For example, the sample of size n_1 switches to n_2 when the sample point S_i falls between w_1 and L_1 (i.e. $w_1 < S_i < L_1$)

and the sample of size n_2 switches to n_1 when the sample point S_i falls below w_2 (i.e. $S_i < w_2$). Figure 2.1 is a graphical view of the VSSI *S* chart.

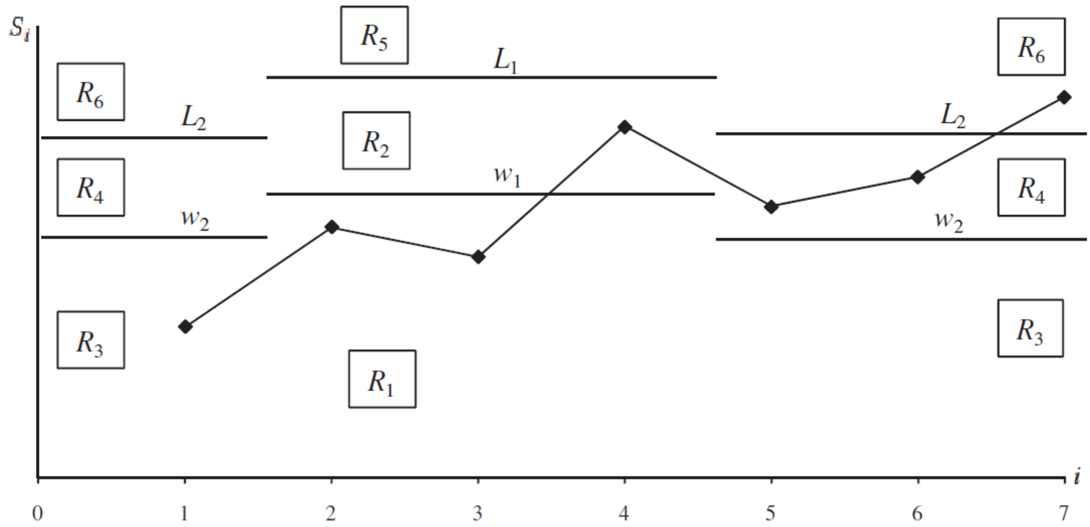

Figure 2.1. Graphical view of a VSSI *S* chart
(Source: Rakitzis and Antzoulakos, 2011)

In Figure 2.1, there are six regions for the VSSI *S* chart. Regions R_1, R_2 and R_5 correspond to adopting the pair of limits (w_1, L_1), while regions R_3, R_4 and R_6 correspond to adopting the pair of limits (w_2, L_2). Rakitzis and Antzoulakos (2011) divided the VSSI *S* chart into three main regions, i.e., the central (regions R_1 and R_3), warning (regions R_2 and R_4) and action (regions R_5 and R_6) regions. The probabilities of S_i falling in the central, warning and action regions are (Rakitzis and Antzoulakos, 2011)

$$P_{0j} = \Pr\left(S_i < w_j \middle| n_j\right) = F_{\chi^2_{n_j-1}}\left(\frac{\left(n_j-1\right)w_j^2}{\left(\lambda\sigma_0\right)^2}\right), \quad (2.8a)$$

$$P_{1j} = \Pr\left(w_j < S_i < L_j \middle| n_j\right) = F_{\chi^2_{n_j-1}}\left(\frac{\left(n_j-1\right)L_j^2}{\left(\lambda\sigma_0\right)^2}\right) - F_{\chi^2_{n_j-1}}\left(\frac{\left(n_j-1\right)w_j^2}{\left(\lambda\sigma_0\right)^2}\right) \quad (2.8b)$$

and

$$P_{2j} = \Pr\left(S_i > L_j \left| n_j \right.\right) = 1 - F_{\chi^2_{n_j-1}}\left(\frac{\left(n_j - 1\right)L_j^2}{\left(\lambda\sigma_0\right)^2}\right), \tag{2.8c}$$

respectively, where $\lambda = \frac{\sigma_1}{\sigma_0}$ is the shift size in the process standard deviation and $F_{\chi^2_{n_j-1}}\left(\cdot\right)$ is the cdf of the chi-square random variable with $n_j - 1$ (for $j = 1, 2$) degrees of freedom. Note that "0" in the subscript of P_{0j} (in Equation (2.8a)) denotes the central region, "1" in the subscript of P_{1j} (in Equation (2.8b)) denotes the warning region, and "2" in the subscript of P_{2j} (in Equation (2.8c)) denotes the action region. Also, note that in Equations (2.8a) – (2.8c), $j = 1$ denotes the previous sample size is n_1, while $j = 2$ denotes the previous sample size is n_2.

Rakitzis and Antzoulakos (2011) defined the time homogeneous Markov chain $\left\{Y_i, i \geq 1\right\}$ with finite state space $\Omega = \left\{1, 2, \ldots, 6\right\}$ for the VSSI *S* chart in Figure 2.1. States 5 and 6 are the absorbing states and $Y_i = t$ if the *i*th sample plotted on the chart, i.e. S_i falls in region R_t (for $t = 1, 2, \ldots, 6$). The initial probability vector is (Rakitzis and Antzoulakos, 2011)

$$\boldsymbol{\pi} = \left[P\left(Y_1 = 1\right), P\left(Y_1 = 2\right), \ldots, P\left(Y_1 = 6\right)\right] = \left(0, 0, P_{02}, P_{12}, 0, P_{22}\right). \tag{2.9}$$

As Rakitzis and Antzoulakos (2011) used the large sample size (i.e. n_2) in taking the first sample (i.e. $i = 1$), $P\left(Y_1 = 1\right) = P\left(Y_1 = 2\right) = P\left(Y_1 = 5\right) = 0$ because regions R_1, R_2 and R_5 are associated with the use of sample size n_1. The probabilities P_{02}, P_{12} and P_{22} are computed from Equations (2.8a), (2.8b) and (2.8c), respectively, using the large sample size n_2. P_{02}, P_{12} and P_{22} are the probabilities that the current sample (S_i) of size n_2 lies in regions R_3, R_4 and R_6, respectively (see Figure 2.1).

The ATS is computed as (Rakitzis and Antzoulakos, 2011)

$$\text{ATS} = t_2 + \boldsymbol{\alpha}\left(\mathbf{I} - \mathbf{Q}\right)^{-1}\mathbf{t}^{\mathrm{T}}, \tag{2.10}$$

where $\boldsymbol{\alpha} = \left(0, 0, P_{02}, P_{12}\right)$ is the initial probability vector for the transient states obtained from vector $\boldsymbol{\pi}$ by removing the last two entries in $\boldsymbol{\pi}$ which correspond to the absorbing states, $\mathbf{I}$ is the identity matrix of order four, $\mathbf{Q}$ is the transition probability matrix given in Equation (2.11) and the vector of sampling intervals is $\mathbf{t} = \left(t_1, t_2, t_1, t_2\right)$. The transition probability matrix (tpm) for the transient states, $\mathbf{Q}$ is (Rakitzis and Antzoulakos, 2011)

$$\mathbf{Q} = \begin{pmatrix} P_{01} & P_{11} & 0 & 0 \\ 0 & 0 & P_{02} & P_{12} \\ P_{01} & P_{11} & 0 & 0 \\ 0 & 0 & P_{02} & P_{12} \end{pmatrix}, \tag{2.11}$$

where the transition probabilities P_{01} and P_{02} are obtained from Equation (2.8a), while P_{11} and P_{12} are obtained from Equation (2.8b). The states 1 and 3 in matrix $\mathbf{Q}$ correspond to regions R_1 and R_3, where the sample size n_1 is used, while the states 2 and 4 in matrix $\mathbf{Q}$ correspond to regions R_2 and R_4, where the sample size n_2 is used.

Rakitzis and Antzoulakos (2011) adopted the large sample size (n_2) in the first sample. However, in the proposed VSSI_t S chart (see Chapter 3), n_0 is used for taking the first sample. In order to ensure a fair comparison between the two charts, a modification is made on the VSSI *S* chart of Rakitzis and Antzoulakos (2011) so that the resulting chart uses n_0 as the first sample. The resulting chart is called the modified VSSI *S* chart hereafter.

The discussion from this paragraph onwards explains the mathematics for the modified VSSI *S* chart that lead to the computation of ATS and EATS. The modified VSSI *S* chart's in-control region is $[0, L)$, where L is the upper control limit. The decision for swapping between the (t_1, n_1) and (t_2, n_2) combinations relies on the value of the current sample standard deviation, S_i. Let w be the warning limit to determine the sample size (n_1 or n_2) and sampling interval (t_1 or t_2) for the next sample $i+1$. Thus, the adaptive function for the modified VSSI *S* chart is

$$\left(t(i+1), n(i+1)\right) = \begin{cases} (t_1, n_1) \text{ if } S_i \in I_1 \\ (t_2, n_2) \text{ if } S_i \in I_2 \end{cases}, \tag{2.12}$$

where $n_1 < n_2$ and $t_1 > t_2$. Figure 2.2 gives a graphical view of the modified VSSI *S* chart.

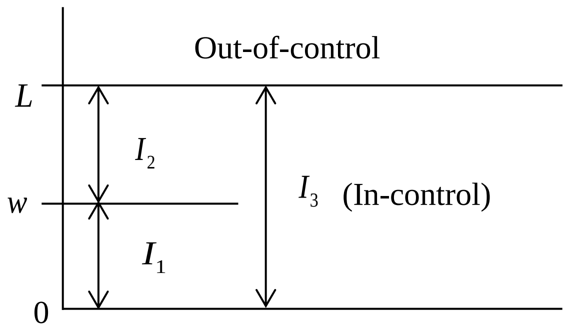

Figure 2.2. Modified VSSI *S* chart

The probabilities of the current sample, S_i, falling in each of the regions I_1, I_2 and I_3 when the process is in-control $(\lambda = 1)$ are given as follows:

$$P(S_i \in I_1) = F_{\chi^2_{n_0-1}}\left(\frac{(n_0 - 1) w^2}{\sigma_0^2}\right), \tag{2.13a}$$

$$P(S_i \in I_2) = F_{\chi^2_{n_0-1}}\left(\frac{(n_0 - 1) L^2}{\sigma_0^2}\right) - F_{\chi^2_{n_0-1}}\left(\frac{(n_0 - 1) w^2}{\sigma_0^2}\right) \tag{2.13b}$$

and

$$P(S_i \in I_3) = F_{\chi^2_{n_0-1}}\left(\frac{(n_0-1)L^2}{\sigma_0^2}\right), \tag{2.13c}$$

where $F_{\chi^2_{n_0-1}}(\cdot)$ is the cdf of a central chi-square random variable with $n_0 - 1$ degrees of freedom. Here, n_0 is a specified desired average sample size when the process is in-control $(\lambda = 1)$. Note that n_0 is related to n_1 and n_2 as follows:

$$n_0 = n_1 \frac{P(S_i \in I_1)}{P(S_i \in I_3)} + n_2 \frac{P(S_i \in I_2)}{P(S_i \in I_3)}. \tag{2.14}$$

By solving Equation (2.14) for w, gives

$$w = \sigma_0 \sqrt{\frac{1}{n_0 - 1} F^{-1}_{\chi^2_{n_0-1}}\left[\frac{n_2 - n_0}{n_2 - n_1} F_{\chi^2_{n_0-1}}\left(\frac{(n_0-1)L^2}{\sigma_0^2}\right)\right]}. \tag{2.15}$$

In like manner, a specified average sampling interval, t_0, when the process is in-control $(\lambda = 1)$, is related to t_1 and t_2 as follows:

$$t_0 = t_1 \frac{P(S_i \in I_1)}{P(S_i \in I_3)} + t_2 \frac{P(S_i \in I_2)}{P(S_i \in I_3)}. \tag{2.16}$$

Note that $P(S_i \in I_1)$, $P(S_i \in I_2)$ and $P(S_i \in I_3)$ in Equations (2.14) and (2.16) are computed using Equations (2.13a), (2.13b) and (2.13c), respectively. Consequently, by solving Equation (2.16) for w, gives

$$w = \sigma_0 \sqrt{\frac{1}{n_0 - 1} F^{-1}_{\chi^2_{n_0-1}}\left[\frac{t_0 - t_2}{t_1 - t_2} F_{\chi^2_{n_0-1}}\left(\frac{(n_0-1)L^2}{\sigma_0^2}\right)\right]}. \tag{2.17}$$

By equating Equations (2.15) and (2.17) and solving for t_1, gives

$$t_1 = \frac{(n_2 - n_1)(t_0 - t_2)}{(n_2 - n_0)} + t_2. \tag{2.18}$$

Thus, for a specified value of t_2, the value of t_1 can be obtained using Equation (2.18).

The performance of the modified VSSI S chart can be measured using the ATS criterion computed as

$$\text{ATS}=\mathbf{b}\left(\mathbf{I}-\mathbf{Q}_*\right)^{-1}\mathbf{t}_*^{\mathrm{T}}, \tag{2.19}$$

where $\mathbf{b}=\left(b_1, b_2\right)$ is the initial vector of starting probabilities such that $b_1+b_2=1$, $\mathbf{I}$ is the identity matrix of order 2, $\mathbf{Q}_*$ is the transition probability matrix (tpm) of the transient states and $\mathbf{t}_*=\left(t_1, t_2\right)$ is the vector of sampling intervals. The tpm $\mathbf{Q}_*$ is given as

$$\mathbf{Q}_*=\begin{pmatrix} Q_{11} & Q_{12} \\ Q_{21} & Q_{22} \end{pmatrix}, \tag{2.20}$$

where

$$Q_{11}=P\left(S_i \in I_1 \middle| n_1; \sigma_1=\lambda\sigma_0\right)=F_{\chi^2_{n_1-1}}\left(\frac{\left(n_1-1\right)w^2}{\left(\lambda\sigma_0\right)^2}\right), \tag{2.21a}$$

$$Q_{12}=P\left(S_i \in I_2 \middle| n_1; \sigma_1=\lambda\sigma_0\right)=F_{\chi^2_{n_1-1}}\left(\frac{\left(n_1-1\right)L^2}{\left(\lambda\sigma_0\right)^2}\right)-F_{\chi^2_{n_1-1}}\left(\frac{\left(n_1-1\right)w^2}{\left(\lambda\sigma_0\right)^2}\right), \tag{2.21b}$$

$$Q_{21}=P\left(S_i \in I_1 \middle| n_2; \sigma_1=\lambda\sigma_0\right)=F_{\chi^2_{n_2-1}}\left(\frac{\left(n_2-1\right)w^2}{\left(\lambda\sigma_0\right)^2}\right) \tag{2.21c}$$

and

$$Q_{22}=P\left(S_i \in I_2 \middle| n_2; \sigma_1=\lambda\sigma_0\right)=F_{\chi^2_{n_2-1}}\left(\frac{\left(n_2-1\right)L^2}{\left(\lambda\sigma_0\right)^2}\right)-F_{\chi^2_{n_2-1}}\left(\frac{\left(n_2-1\right)w^2}{\left(\lambda\sigma_0\right)^2}\right). \tag{2.21d}$$

Note that b_1 and b_2 are the proportions of time spent using $\left(t_1, n_1\right)$ and $\left(t_2, n_2\right)$, respectively (Prabhu et al., 1994). Hence, the formulae for computing b_1 and b_2 are

$$b_1 = \frac{P(S_i \in I_1)}{P(S_i \in I_3)} \tag{2.22a}$$

and

$$b_2 = \frac{P(S_i \in I_2)}{P(S_i \in I_3)}, \tag{2.22b}$$

respectively. The expected average time to signal (EATS) is one of the performance criteria used in this thesis. The EATS of the modified VSSI *S* chart is obtained as (Khaw et al., 2017)

$$\text{EATS} = E\left[\text{ATS}(\lambda)\right] = \int_{\lambda_{\min}}^{\lambda_{\max}} \text{ATS}(\lambda)\, f(\lambda)\, d\lambda\,. \tag{2.23}$$

Here, $f(\lambda)$ denotes the pdf of the shift size, λ, where λ is assumed to follow a uniform, $U(\lambda_{\min}, \lambda_{\max})$ distribution. Note that $\lambda_{\min}$, $\lambda_{\max}$ and $f(\lambda)$ have been defined in Section 2.2.

2.4 Exponentially Weighted Moving Average (EWMA) *S* Chart

Crowder and Hamilton (1992) proposed the EWMA *S* chart by employing the smoothing technique on the *S* chart. The performance of the EWMA *S* chart is better than the usual range chart (*R* chart) or variance chart (S^2 chart) in detecting small shifts in the process standard deviation. The logarithm of the sample variance is used in the EMWA *S* chart to monitor the process standard deviation. This is because the distribution of $\ln(S^2)$ is more symmetric than that of S^2 (Knoth., 2005). Although the control limits of the EWMA chart are not as easy to set up as that of an *S* chart, the EWMA chart can be a good alternative due to its good performance in detecting small shifts (Adeoti and Olaomi, 2016).

Let $\ln\left(S^2\right)$, where S^2 is the usual sample variance. The statistic for the EWMA *S* chart is (Crowder and Hamilton, 1992)

$$EWMA_i = \max\left\{\left(1-\lambda^*\right)EWMA_{i-1} + \lambda^* y_i, \ln\left(\sigma_0^2\right)\right\}, \text{ for } i = 1, 2, \ldots, \qquad (2.24)$$

where $EWMA_0 = \ln\left(\sigma_0^2\right)$, λ^* is a smoothing constant satisfying $0 < \lambda^* \leq 1$ and $y_i = \ln\left(S_i^2\right)$, where S_i^2 denotes the successive sample variances. Note that in Equation (2.24), $\max\left(a,b\right)$ denotes the maximum value between a and b. The upper control limit (UCL) of the upper-sided EWMA *S* chart is (Crowder and Hamilton, 1992)

$$\text{UCL} = \ln\left(\sigma_0^2\right) + K\sigma_{EWMA}, \qquad (2.25)$$

where

$$\sigma_{EWMA} = \sqrt{\left(\frac{\lambda^*}{2-\lambda^*}\right)\text{Var}\left\{\ln\left(S_i^2\right)\right\}}. \qquad (2.26)$$

Since $\text{Var}\left\{\ln\left(S_i^2\right)\right\}$ is a trigamma function, by using the infinite series of expansion and solving approximately for $\text{Var}\left\{\ln\left(S_i^2\right)\right\}$, gives (Crowder and Hamilton, 1992)

$$\text{Var}\left\{\ln\left(S_i^2\right)\right\} = \frac{2}{n-1} + \frac{2}{\left(n-1\right)^2} + \frac{4}{3\left(n-1\right)^3} - \frac{16}{15\left(n-1\right)^5}. \qquad (2.27)$$

Crowder and Hamilton (1992) provided the integral equation approach to design the EWMA *S* chart. However, for consistency, the Markov chain approach is applied in the optimal design of the EWMA *S* chart in this thesis. The in-control region of the EMWA *S* chart is divided into $m = 100$ equally spaced subintervals. The ARL of the EWMA *S* chart is

$$\text{ARL} = \mathbf{b}\left(\mathbf{I}-\mathbf{Q}\right)^{-1}\mathbf{1}^{\text{T}}, \qquad (2.28)$$

where $\mathbf{b} = (1, 0, \ldots, 0)_{1\times m}$ is the initial probability vector, $\mathbf{I}$ is the identity matrix with dimension $m\times m$, $\mathbf{Q}$ is the tpm for the transient states with dimension $m\times m$ and $\mathbf{1}^{\mathrm{T}}$ is a $m\times 1$ vector of all ones. The entry Q_{jk} of matrix $\mathbf{Q}$ is the transition probability given by

$$Q_{jk} = F_G\left(e^{\frac{\left(k-0.5-\left(1-\lambda^*\right)(j-1)\right)w}{\lambda^*}} \middle| \frac{n_0-1}{2}, \frac{2\sigma_0^2}{n_0-1} \right) - F_G\left(e^{\frac{\left(k-1.5-\left(1-\lambda^*\right)(j-1)\right)w}{\lambda^*}} \middle| \frac{n_0-1}{2}, \frac{2\sigma_0^2}{n_0-1} \right), \quad (2.29)$$

where $j = 1, 2, \ldots, m$ and $k = 2, 3, \ldots, m$. However, for $j = 1, 2, \ldots, m$ and $k = 1$,

$$Q_{j1} = F_G\left(e^{\frac{\left(0.5-\left(1-\lambda^*\right)(j-1)\right)w}{\lambda^*}} \middle| \frac{n_0-1}{2}, \frac{2\sigma_0^2}{n_0-1} \right). \quad (2.30)$$

Note that $w = \frac{2\left(\mathrm{UCL}-\mathrm{CL}\right)}{2m-1}$ and $F_G\left(\cdot \middle| \frac{n_0-1}{2}, \frac{2\sigma_0^2}{n_0-1} \right)$ is the cdf of the gamma $G\left(\frac{n_0-1}{2}, \frac{2\sigma_0^2}{n_0-1} \right)$ distribution, where n_0 is the fixed sample size. The formula to compute the EARL of the EWMA *S* chart is (Huh, 2014)

$$\mathrm{EARL} = E\left[\mathrm{ARL}(\lambda)\right] = \int_{\lambda_{\min}}^{\lambda_{\max}} \mathrm{ARL}(\lambda)\, f(\lambda)\, d\lambda . \quad (2.31)$$

Here, $f(\lambda)$ denotes the pdf of the shift size λ, where λ is assumed to follow a uniform, $U(\lambda_{\min}, \lambda_{\max})$ distribution. Note that $\lambda_{\min}$ and $\lambda_{\max}$ have been defined in Section 2.2.

The optimal design of the EWMA *S* chart in this thesis is based on minimizing the ATS_1, or similarly the ARL_1, as $\mathrm{ATS}_1 = \mathrm{ARL}_1$ for the EWMA *S* chart which adopts the fixed sampling interval $t_0 = 1$. The out-of-control shift sizes in the process standard deviation, where a quick detection is needed, considered are

$\lambda \in \{1.1, 1.2, \ldots, 2\}$. Note that $\lambda = \frac{\sigma_1}{\sigma_0}$, where σ_0 and σ_1 are the in-control and out-of-control process standard deviations, respectively. The optimization procedure of the EWMA *S* chart, for minimizing the shift size, λ, is summarized as follows:

Step 1. Specify n_0, $\text{ATS}_0 \left(= \text{ARL}_0\right)$ and the shift size λ, for which a quick detection is needed.

Step 2. Initialize $\lambda^* = 0.01$. Determine the value of K using the bisection method to satisfy the ATS_0 value specified in Step 1.

Step 3. If $\lambda^* \leq 1.0$, increase λ^* by 0.01 and return to Step 2 to compute K. Otherwise, proceed to Step 4.

Step 4. For each combination of $\left(\lambda^*, K\right)$, compute the corresponding ATS_1 $\left(= \text{ARL}_1\right)$ value, for the shift size λ, using Equation (2.28). Then select the $\left(\lambda^*, K\right)$ combination that gives the minimum ATS_1 value, for the shift size λ.

In a similar manner (by using the above Steps 1 – 4), the optimal parameters $\left(\lambda^*, K\right)$ that minimize the EATS_1 value for the shift interval $\left(\lambda_{\text{min}}, \lambda_{\text{max}}\right)$ of the EWMA *S* chart in this thesis can be obtained. The only differences are (i) ATS_0 in Steps 1 and 2 are replaced by EATS_0, (ii) ATS_1 in Step 4 is replaced by EATS_1 and (iii) λ in Steps 1 and 4 is substituted for $\left(\lambda_{\text{min}}, \lambda_{\text{max}}\right)$.

2.5 Summary

An overview of the standard *S* chart and the use of probability limits in computing the chart's UCL are given in this chapter. In addition, a modification of the existing VSSI *S* chart, as well as the Markov chain model of the chart is enumerated. The VSSI *S* chart is modified so that the chart's initial sample size can be set to be similar to that of the VSSI_t *S* chart proposed in Chapter 3. This will enable a fair performance comparison between the two charts. The Markov chain design of the EWMA *S* chart is also presented. The following chapter discusses the Markov chain model and optimal design of the proposed VSSI_t *S* chart.

CHAPTER 3

A PROPOSED IMPROVED VARIABLE SAMPLE SIZE AND SAMPLING INTERVAL (VSSI_t) *S* CONTROL CHART

3.1 Introduction

In this chapter, the proposed VSSI_t S chart is discussed. The construction of the VSSI_t S chart is motivated by the existing improved VSSI $\bar{X}$ (called the VSSI_t $\bar{X}$) chart of Noorossana et al. (2016), where the VSSI_t $\bar{X}$ chart improves upon the performance of the standard VSSI $\bar{X}$ chart in detecting shifts in the process mean. Likewise, the proposed VSSI_t S chart is expected to outperform the existing VSSI *S* chart. A similar Markov chain approach adopted by Noorossana et al. (2016), for the VSSI_t $\bar{X}$ chart, is used to design the VSSI_t S chart. The optimal design of the VSSI_t S chart is presented in Section 3.4, where the steps are provided to compute the optimal parameters for minimizing the out-of-control ATS (ATS_1), based on a specified shift size in the process standard deviation, where a quick detection is important.

3.2 Some Background Discussion

The Shewhart *S* chart is used to guard against shifts in the process standard deviation. The occurrence of shifts in the process standard deviation will decrease the capability of the process in producing quality output. Similar to the Shewhart $\bar{X}$ chart, the *S* chart is easy to use and able to detect a large shift in the process standard deviation quickly. However, it is insensitive in detecting small shifts in the process standard deviation (Lee et al., 2012).

In order to increase the sensitivity of a chart towards small and moderate shifts, several adaptive features, such as the variable sampling interval (VSI) and variable sample size (VSS) features are incorporated into the basic chart at hand. According to the value of the current sample statistic, the VSI feature allows the length of the sampling interval between the current and the next samples to vary while the VSS feature allows the sample size to vary. A simultaneous use of the VSI and VSS features on a control chart leads to the development of the variable sample size and sampling interval (VSSI) control chart (Rakitzis and Antzoulakos, 2011).

Noorossana et al. (2016) proposed the modified variable sample size and sampling interval (VSSI_t) $\bar{X}$ chart, which is obtained by modifying the VSSI $\bar{X}$ chart of Prabhu et al. (1994) by adding an additional sampling interval. Thus, the VSSI_t $\bar{X}$ chart has two sample sizes and three sampling intervals. Noorossana et al. (2016) showed that the VSSI_t $\bar{X}$ chart outperforms the VSI, VSS and VSSI $\bar{X}$ charts. By extending the design of the VSSI_t $\bar{X}$ chart to the case of monitoring the process standard deviation, this thesis discusses the construction of an improved VSSI *S* (called VSSI_t S) chart. In line with the superiority of the VSSI_t $\bar{X}$ chart for monitoring the process mean, the VSSI_t S chart prevails over the existing *S*-type charts for monitoring the process standard deviation.

3.3 Markov Chain Model for the VSSI_t S Chart

Noorossana et al. (2016) considered the VSSI_t scheme that uses two different sample sizes (n_1, n_2), three different sampling intervals (t_1, t_2, t_3), a pair of warning limits (w_1, w_2) and a control limit (k_0), where $w_1 < w_2 < k_0$. As only the upper-sided portion of the chart is considered, the in-control region is $[0, k_0)$. The in-control region is further divided into three intervals, namely $I_1 = [0, w_1)$, $I_2 = [w_1, w_2)$ and $I_3 = [w_2, k_0)$. Figure 3.1 shows a graphical view of the VSSI$_t$ S chart with the intervals I_1, I_2 and I_3. Figure 3.1 comprises an additional region compared to Figure 2.2. By having more regions, more sample size and sampling interval combinations can be assigned to the said regions, hence, making the VSSI$_t$ S chart more sensitive than the modified VSSI S chart, in detecting shifts in the process standard deviation.

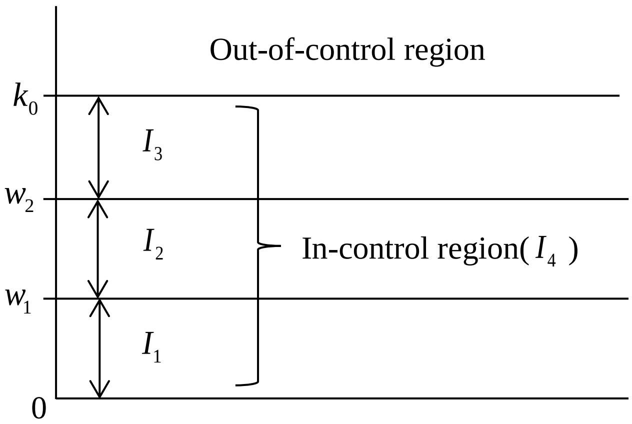

Figure 3.1. VSSI$_t$ S chart

The rule for switching between n_1 and n_2, and among t_1, t_2 and t_3, based on where the current sample S_i plots on the chart is given as follows:

$$(t(i+1), n(i+1)) = \begin{cases} (t_1, n_1) & \text{if } S_i \in I_1 \\ (t_2, n_1) & \text{if } S_i \in I_2 \\ (t_3, n_2) & \text{if } S_i \in I_3 \end{cases}, \quad (3.1)$$

where $n_1 < n_2$, $t_1 > t_2 > t_3$ and the notations $t(i+1)$ and $n(i+1)$ are defined in Section 2.3. The process standard deviation is very unlikely to change when the current sample point lies in I_1. Therefore, the small sample size n_1 is used with the long sampling interval t_1. When the current sample point lies in I_2, the moderate sampling interval t_2 is used for a quicker detection of a possible shift but the small sample size n_1 is adopted. The short sampling interval t_3 and large sample size n_2 are used when the current sample point lies in I_3 so that if the process standard deviation shifts to an out-of-control state, the shift can be detected as quickly as possible.

Let P_1 denote the probability that S_i lies in I_1 given that the prior sample, S_{i-1} lies in I_4, where $I_4 = [0, k_0)$ is the in-control region. Also, let P_2 and P_3 be the probabilities that S_i lies in I_2 and I_3, respectively, given that S_{i-1} lies in I_4. The formulae for probabilities P_1 , P_2 and P_3 when the process is in-control, i.e. $\lambda = 1$ so that $\sigma_1 = \sigma_0$, are given as follows:

$$P_1 = P\left(S_i \in I_1 \middle| S_{i-1} \in I_4, \lambda = 1\right) = \frac{F_{\chi^2_{n_0-1}}\left(\frac{(n_0 - 1)w_1^2}{\sigma_0^2}\right)}{F_{\chi^2_{n_0-1}}\left(\frac{(n_0 - 1)k_0^2}{\sigma_0^2}\right)}, \quad (3.2a)$$

$$P_2 = P\left(S_i \in I_2 \middle| S_{i-1} \in I_4, \lambda = 1\right) = \frac{F_{\chi^2_{n_0-1}}\left(\frac{(n_0 - 1)w_2^2}{\sigma_0^2}\right) - F_{\chi^2_{n_0-1}}\left(\frac{(n_0 - 1)w_1^2}{\sigma_0^2}\right)}{F_{\chi^2_{n_0-1}}\left(\frac{(n_0 - 1)k_0^2}{\sigma_0^2}\right)} \quad (3.2b)$$

and

$$P_3 = P\left(S_i \in I_3 \middle| S_{i-1} \in I_4, \lambda = 1\right) = \frac{F_{\chi^2_{n_0-1}}\left(\frac{(n_0 - 1)k_0^2}{\sigma_0^2}\right) - F_{\chi^2_{n_0-1}}\left(\frac{(n_0 - 1)w_2^2}{\sigma_0^2}\right)}{F_{\chi^2_{n_0-1}}\left(\frac{(n_0 - 1)k_0^2}{\sigma_0^2}\right)}, \quad (3.2c)$$